Femtosecond-laser inscribed double-cladding waveguides in Nd:YAG crystal: a promising prototype for integrated lasers

Hongliang Liu,[1] Feng Chen,[1,*] Javier R. Vázquez de Aldana,[2] and D. Jaque[3]

[1]*School of Physics, State Key Laboratory of Crystal Materials and Key Laboratory of Particle Physics and Particle Irradiation (Ministry of Education), Shandong University, Jinan 250100, China*

[2]*Laser Microprocessing Group, Universidad de Salamanca, Salamanca 37008, Spain*

[3]*Fluorescence Imaging Group, Departamento de Física de Materiales, Facultad de Ciencias, Universidad Autónoma de Madrid, Madrid 28049, Spain*

**Corresponding author: drfchen@sdu.edu.cn*

Received July 16, 2013; revised July 30, 2013; accepted July 30, 2013; posted July 31, 2013 (Doc. ID 194061); published August 22, 2013

We report on the design and implementation of a prototype of optical waveguides fabricated in Nd:YAG crystals by using femtosecond-laser irradiation. In this prototype, two concentric tubular structures with nearly circular cross sections of different diameters have been inscribed in the Nd:YAG crystals, generating double-cladding waveguides. Under 808 nm optical pumping, waveguide lasers have been realized in the double-cladding structures. Compared with single-cladding waveguides, the concentric tubular structures, benefiting from the large pump area of the outermost cladding, possess both superior laser performance and nearly single-mode beam profile in the inner cladding. Double-cladding waveguides of the same size were fabricated and coated by a thin optical film, and a maximum output power of 384 mW and a slope efficiency of 46.1% were obtained. Since the large diameters of the outer claddings are comparable with those of the optical fibers, this prototype paves a way to construct an integrated single-mode laser system with a direct fiber-waveguide configuration.

OCIS codes: (230.7370) Waveguides; (160.3380) Laser materials; (140.3390) Laser materials processing.
http://dx.doi.org/10.1364/OL.38.003294

Light in optical waveguides can reach high optical intensities owing to the confinement of the light field within much more compact volumes; consequently, laser oscillations in active gain waveguides may possess low lasing thresholds and comparable efficiency with respect to the bulk lasers [1,2]. In addition, a single photonic chip may be constructed in waveguide platforms to achieve multiple functions [3,4]. Since 1996, femtosecond (fs) laser inscription has become a powerful technique for microstructuring of various optical materials, and a wide range of photonic applications have been realized [4–14]. These guiding structures include the single-line written waveguides (so-called type I, with positive refractive index changes in the irradiated filament) [8], double-line fabricated waveguides (so-called type II, with stress-induced guiding region between the two tracks of negative index changes) [9–14], and depressed cladding waveguides (located in the core surrounded by multiple low-index tracks) [15–18]. In Nd:YAG laser crystals, both type-II stress-induced waveguides [14] and depressed single-cladding waveguides [17,18] have been successfully fabricated with fs pulses. One of the advantages of the cladding waveguides is that the large-scale cross sections match the commercially available multimode fibers (with diameters of 100–400 μm), which in principle offers an opportunity to realize efficient fiber-waveguide laser systems with low costs. However, as a drawback, the cladding waveguide lasers usually show multimodal beam properties due to the large diameters of the structures [19]. The type-II stress-induced waveguides exhibit single-mode features; however, the efficient pump of such structures relies on tightly focused beams (of diameters no more than 20 μm), which cannot be achieved directly from fiber-coupled high-power diode lasers (usually out-coupled by multimode fibers with diameters of 100–400 μm) [20].

In this Letter, we propose a configuration of double-cladding waveguides containing two concentric tubes with different diameters, which is, to some extent, similar to double-cladding fibers. Furthermore, spatial distribution of the lattice residual stress (as obtained from spectral shifts), fluorescence efficiency, and fluorescence linewidth were measured in an area covering the cladding waveguide. The generated waveguide lasers are found to behave as nearly single-mode, delivering higher output powers, compared with the single-cladding waveguides.

The optically polished Nd:YAG crystal used in this work was cut into dimensions of $8\ mm \times 10\ mm \times 2\ mm$. The double-cladding waveguides with circular boundaries were produced by using the laser facility of Universidad de Salamanca, Spain. Figure 1(a) shows the scheme of the fs-laser fabrication procedure in the Nd:YAG crystal. We used an amplified Ti:sapphire laser system generating linearly polarized 120 fs pulses at a central wavelength of 800 nm (with 1 kHz repetition rate and 1 mJ maximum pulse energy). The pulse energy used to irradiate the sample was set with a calibrated neutral density filter, a half-wave plate, and a linear polarizer. The sample was placed in a computer-controlled motorized three-axes stage. The beam was focused through the largest sample surface (dimensions $8\ mm \times 10\ mm$) at a depth of 150 μm through a microscope objective (Leica 40×, numerical aperture NA = 0.65) with a pulse energy of 0.2 μJ. The linear and nonlinear refractive indices of YAG are $n_0 = 1.83$ and $n_2 \approx 6 \times 10^{-16}$ cm^2/W. Based on these values the YAG threshold power for self-focusing has been estimated previously to be 0.9 MW. The laser

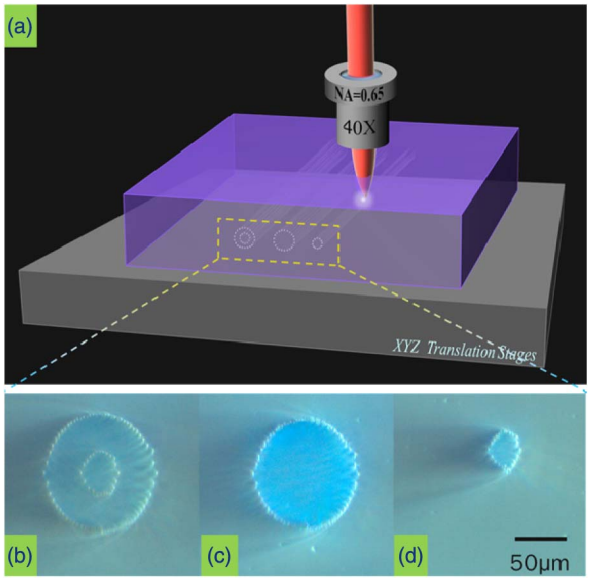

Fig. 1. (a) Fabrication schematic of fs-laser inscription process in Nd:YAG crystals, and optical images of (b) double-cladding waveguides and single-cladding waveguides with diameters of (c) 100 and (d) 30 μm.

power used in our experiments is estimated to be, for the pulse energy of 0.2 μJ, close to 1.5 MW, which is above the YAG threshold power for self-focusing, and hence self-focusing is expected to occur, leading to the creation of elongated damage tracks. During the irradiation, the sample was moved at a constant speed of 700 μm/s in the direction perpendicular to the laser polarization and the pulse propagation, which was carefully aligned with the 10-mm-long edge of the sample, thus producing a damage track along the sample. Many parallel scans (with ~3 μm separation between adjacent damage tracks) were performed at different depths of the sample (from bottom to top in order to avoid the shielding of the incident pulses by the previously written damage tracks) to inscribe the double-cladding waveguide, which consisted of a tubular central structure with 30 μm diameter, and concentric larger size tubular claddings (100 μm diameter). The cross section of the resulting structures in the Nd:YAG crystal can be seen in Fig. 1(b). For comparison, single-cladding waveguides with cross-section diameters of 100 and 30 μm [see Figs. 1(c) and 1(d)] were produced in the same crystal. The propagation losses of the waveguides at 633 nm were about 1.9, 1.7, and 2.0 dB/cm at TE polarization, respectively.

The ultrafast laser inscription produced obvious modifications of the microstructural and fluorescent properties in the filaments (fs-laser focus), as clearly illustrated in the fluorescence images included in Fig. 2, which correspond to the concentric tubular configuration. The graphs correspond to the spatial distribution of the residual stress affecting the Nd:YAG network pressure (as obtained from the induced spectral shifts of fluorescence lines and that are given in kBar units), the FWHM (in cm^{-1} units), and the intensity (in a.u. units) of the $^4F_{3/2} \rightarrow {}^4I_{9/2}$ inter-Stark level emission line of Nd^{3+} ions around 940 nm (this line is used for this analysis since it has been found to be hypersensitivity to slight changes in the Nd^{3+} environments, for example, strain, volume

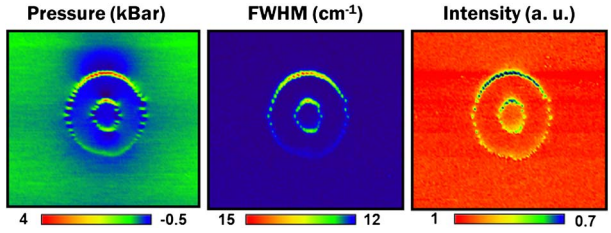

Fig. 2. Spatial distributions of (a) pressure, (b) FWHM, and (c) intensity corresponding to the $^4F_{3/2} \rightarrow {}^4I_{9/2}$ inter-Stark level emission line of Nd^{3+} in the double-cladding waveguide.

changes, and disorder). As we can see, a compressive stress is created along the waveguide contour, being as large as 4 kBar. The spatial variation of the linewidth reveals a large broadening of the fluorescence lines at waveguide contour, which is proportional to the former one. This, indeed, could be attributed to the local disorder of the Nd:YAG system as a consequence of the damage caused by the tightly focused fs laser. Finally, the image about the fluorescence intensity (revealing a net reduction at the damage focus) unequivocally reveals the creation of defects induced at these locations (i.e., partially damaged areas). According to the previous work [21], the light is confined within the structures as a consequence of the lower barrier caused by the localized damage. Therefore, the fluorescence images included in Fig. 2 show a strong modification of the Nd:YAG system, caused by simultaneous damage, compression, and disorder, only at the waveguide's contour in the cladding waveguides. Nevertheless, the Nd:YAG network with slight modification at the waveguide volume leads to a partial dilatation that is not accompanied by any relevant disorder or damage. With the consistency of the focus, where the refractive index decreases consecutively measured about 3×10^{-3}, the concentric tubular cladding waveguide could confine the light intensively propagating in the structure.

The continuous-wave (cw) laser experiments were performed by using an end-face coupling system. A tunable cw Ti:sapphire laser (Coherent MBR 110) generated a polarized light pump beam at 808 nm. A spherical convex lens with a focal length of 70 mm was used to focus the pump beam, reducing it to a diameter of ~140 μm and coupling it into the waveguide. To achieve the Fabry–Perot cavity for the 1.06 μm laser emission in the waveguides, two dielectric mirrors were butt-coupled to the two polished end facets [the input one with a high reflectivity (>99%) at 1.06 μm and high transmission (98%) at 808 nm and the output one with reflectivity of 60% at 1.06 μm and >99% at 808 nm]. The generated waveguide lasers were collected with a 20× microscope objective lens (NA = 0.4) and imaged by an IR CCD camera through an aperture. A spectrometer was used to analyze the emission spectra of the generated laser beam. In the laser experiments, the double-cladding waveguides showed stable and remarkable performance.

The near-field intensity profiles of the output lasers from the double-cladding waveguide and single-cladding waveguides at 1064 nm are depicted in Figs. 3(d)–3(f). For comparison, Figs. 3(a)–3(c) show the multimode near-field intensity distribution at 632.8 nm from the

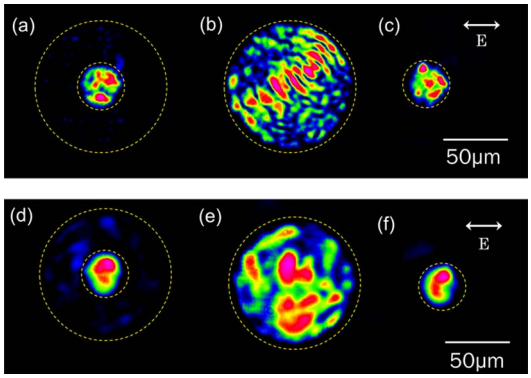

Fig. 3. Near-field intensity profiles of the TE mode of the laser for the waveguides at (a)–(c) 632.8 nm and (d)–(f) 1064 nm.

inner core of the double-cladding waveguide and the single-cladding waveguides with diameters of 100 and 30 μm, respectively. As one can see, the 30-μm-diameter cladding structures, i.e., in both the inner core of the double cladding and that of the single-cladding [see Figs. 3(d) and 3(f)] supported single-mode waveguide lasers, which is significantly different from the larger-scale claddings [see Fig. 3(e)]. It should be pointed out that, different from the type-II Nd:YAG waveguides [14], the laser performances as well as the guidance features from these cladding waveguides are similar for both TE and TM polarizations, which shows good flexibility for a normal diode laser pump.

Figure 4 shows the output power of generated lasers at 1064 nm as a function of absorbed pump power at 808 nm obtained from the inner 30-μm-diameter core of the double-cladding waveguides and the single-cladding waveguides with diameters of 100 and 30 μm, respectively. The inset graph shows the spectrum of the laser oscillation at 1064 nm corresponding to the $^4F_{3/2} \rightarrow {}^4I_{11/2}$ emission line of the Nd^{3+} ions, with the FWHM being 0.5 nm. From the linear fits of the output power as a function of the absorbed power, a slope efficiency of 38.9% can be obtained from the inner core of double-cladding waveguides. In addition, the obtained maximum output power of the 1064 nm lasers was 102 mW from the double-cladding (inner mode) waveguide when the absorbed power was 350 mW. And the lasing thresholds were determined to be 103 mW. For a good comparison, the laser curves of the single-cladding structures were depicted in the figure. We obtained waveguide lasers with slope efficiencies of 26% and 21% for the single-cladding structures with diameters of 100 and 30 μm, respectively. These values are considerably lower than those from the double-cladding waveguide core. Moreover, the lasing thresholds of the single claddings with a diameter of 100 μm were 256 mW, which was higher than that of the double-cladding core. More importantly, the maximum output powers of the 30 μm nearly single-mode waveguide lasers from the double-cladding cores are as high as 102 mW, which is 50% higher than that of the 30 μm single-cladding structure (68 mW) with similar threshold. This owes to the large-area pump but compressed output volume, which means that more pumping light goes into the whole structure but only generates guided IR lasers in the inner core region. This advantage of the double-cladding structures reflects on the laser performances, resulting in reduced lasing thresholds, higher slope efficiencies, and increased output powers.

Concentric larger size tubular claddings with diameter of 100 μm and an inner waveguide core with diameter of 30 μm were fabricated with a pulse energy of 0.42 μJ. A thin film with a high reflectivity at 1.06 μm and high transmission at 808 nm was coated (serving as the input mirror) on the sample to form the laser resonance cavity with the end-face of the crystal. The laser experiment was performed under the same conditions without using an output mirror at room temperature. From the linear fit of the data shown in Fig. 5, the maximum output power obtained are 346 and 384 mW for the waveguide laser at TM and TE polarization, respectively. The inset graph shows the generated single mode of the laser supported both at TE and TM polarization. The slope efficiencies are 41.5% and 46.1%, respectively, which are quite higher than those obtained for the sample without thin film. Meanwhile, from comparison of the laser performance as depicted in Table 1, this experiment certified that the effect of using thin film to form the laser resonant

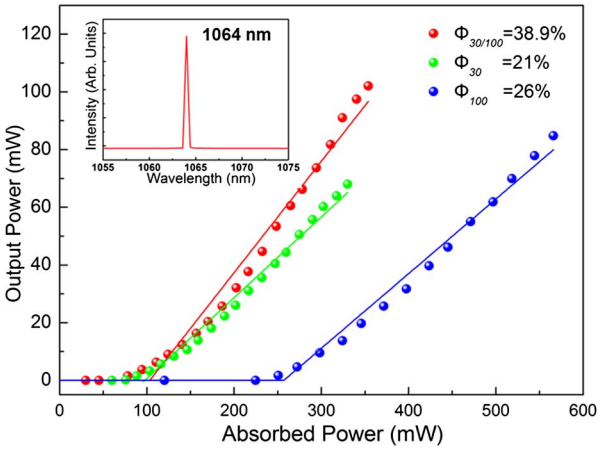

Fig. 4. Output power of the generated lasers at 1064 nm as a function of the absorbed pump power at 808 nm. The inset graph shows the spectrum of the laser at 1064 nm (0.5 nm FWHM).

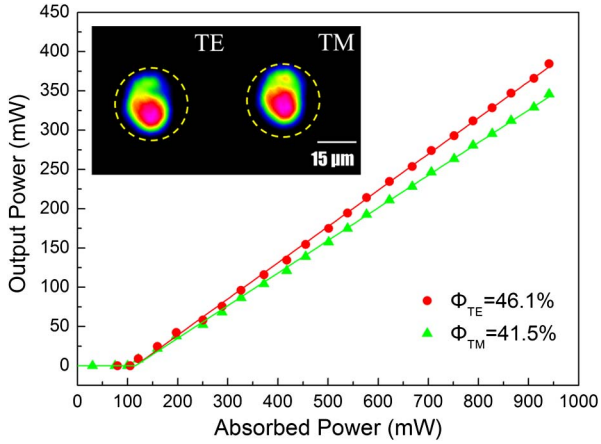

Fig. 5. Output power of the laser as a function of the absorbed power at room temperature. The inset graph displays the laser mode of the laser from the waveguide cores at both TE and TM polarization.

Table 1. Characteristics of Double-Cladding Waveguides

Polarization Direction	Mirror/Film	Output Power (Max.) (mW)	Slope Efficiency (%)	Lasing Threshold (mW)
TE	Mirror	102	38.9	101
TM	Mirror	91	32	104
TE	Film	384	46.1	106
TM	Film	346	41.5	105

cavity is much more efficient than using additional mirrors, with an improvement of the optical conversion efficiency from 28.6% to 41% at TE mode.

In conclusion, we have fabricated concentric tubular waveguides with double claddings in Nd:YAG crystal by using fs-laser inscription. Nearly single-mode waveguide lasers with slope efficiency of 46.1% and maximum output power of 384 mW from the inner cores have shown superior laser performance to the standard single-cladding waveguides, which benefits from the large-area pump of the outermost cladding. It should also be pointed out that the laser performances of the cladding waveguides in the present work are limited by the powers of the pumping lasers. A few watts output power of the generated waveguide lasers could be expected in the case of an efficient pump from a fiber-coupled diode laser. In addition, since one of the major advantages of the fs-laser writing technique is the capability of realizing arbitrary shapes, it is intriguing to produce more complicated geometry (e.g., D-shaped cladding with off-centered core) to improve the lasing performances. This work paves a new way toward constructing an integrated high-power, single-mode laser system with a direct fiber-waveguide configuration.

This work was supported by the National Natural Science Foundation of China (Grant No. 11274203) and the Spanish Ministerio de Ciencia e Innovación (MICINN) through Consolider Program SAUUL CSD2007-00013 and project FIS2009-09522. Support from the Centro de Láseres-Pulsados (CLPU) is also acknowledged.

References

1. C. Grivas, Prog. Quantum Electron. **35**, 159 (2011).
2. F. Chen, Laser Photon. Rev. **6**, 622 (2012).
3. W. Sohler, H. Hu, R. Ricken, V. Quiring, C. Vannahme, H. Herrmann, D. Büchter, S. Reza, W. Grundkötter, S. Orlov, H. Suche, R. Nouroozi, and Y. H. Min, Opt. Photon. News **19**(1), 24 (2008).
4. J. Thomas, M. Heinrich, P. Zeil, V. Hilbert, K. Rademaker, R. Riedel, S. Ringleb, C. Dubs, J.-P. Ruske, S. Nolte, and A. Tünnermann, Phys. Status Solidi A **208**, 276 (2011).
5. K. M. Davis, K. Miura, N. Sugimoto, and K. Hirao, Opt. Lett. **21**, 1729 (1996).
6. M. Ams, G. D. Marshall, P. Dekker, J. Piper, and M. Withford, Laser Photon. Rev. **3**, 535 (2009).
7. R. R. Gattass and E. Mazur, Nat. Photonics **2**, 219 (2008).
8. J. Burghoff, S. Nolte, and A. Tunnermann, Appl. Phys. A **89**, 127 (2007).
9. G. A. Torchia, P. F. Meilan, A. Rodenas, D. Jaque, C. Mendez, and L. Roso, Opt. Express **15**, 13266 (2007).
10. Y. Tan, F. Chen, J. R. Vázquez de Aldana, G. A. Torchia, A. Benayas, and D. Jaque, Appl. Phys. Lett. **97**, 031119 (2010).
11. C. Zhang, N. Dong, J. Yang, F. Chen, J. R. Vázquez de Aldana, and Q. Lu, Opt. Express **19**, 12503 (2011).
12. T. Calmano, J. Siebenmorgen, F. Reichert, M. Fechner, A. Paschke, N. Hansen, K. Petermann, and G. Huber, Opt. Lett. **36**, 4620 (2011).
13. C. Grivas, C. Corbari, G. Brambilla, and P. Lagoudakis, Opt. Lett. **37**, 4630 (2012).
14. T. Calmano, J. Siebenmorgen, O. Hellmig, K. Petermann, and G. Huber, Appl. Phys. B **100**, 131 (2010).
15. D. G. Lancaster, S. Gross, H. Ebendorff, K. Kuan, M. Ams, and M. Withford, Opt. Lett. **36**, 1587 (2011).
16. D. G. Lancaster, H. Ebendorff, A. Fuerbach, M. J. Withford, and T. M. Monro, Opt. Lett. **37**, 996 (2012).
17. A. Okhrimchuk, V. Mezentsev, A. Shestakov, and I. Bennion, Opt. Express **20**, 3832 (2012).
18. H. Liu, Y. Jia, J. R. Vázquez de Aldana, D. Jaque, and F. Chen, Opt. Express **20**, 18620 (2012).
19. R. Ramponi, R. Osellame, and M. Marangoni, Rev. Sci. Instrum. **73**, 1117 (2002).
20. F. Chen and J. R. Vázquez de Aldana, "Optical waveguides in crystalline dielectric materials produced by femtosecond-laser micromachining," Laser Photon. Rev., doi:10.1002/lpor.201300025 (2013).
21. A. Ródenas, G. A. Torchia, G. Lifante, E. Cantelar, J. Lamela, F. Jaque, L. Roso, and D. Jaque, Appl. Phys. B **95**, 85 (2009).